Multiphase flow models for 2D numerical modeling of flow over spillways

D. Kositgittiwong[1], C. Chinnarasri[1], P.Y. Julien[2], J.F. Ruff[2] & R.N. Meroney[2]
[1] *Water Resources Engineering Research Lab. (WAREE), Department of Civil Engineering, King Mongkut's University of Technology Thonburi, Bangkok, THAILAND. e-mail:chaiyuth.chi@kmutt.ac.th*
[2] *Department of Civil and Environmental Engineering, Colorado State University, CO, US*

ABSTRACT**:** Stepped spillways are becoming increasingly popular due to the low-cost in construction and high efficiency. Numerical modeling of stepped spillways is very complicated and challenging because of the high roughness and velocity recirculation regions. Two types of multiphase flow models are used: a mixture multiphase flow model (MMF) and a volume of fluid multiphase flow model (VOF). The differences between both models are the phases interpenetrating and the phase velocities. In both models, the realizable k-ε model is chosen to simulate turbulence. The computational results are compared with large-scale experimental data from Colorado State University. The spillway was 1.22m wide and consisted of 25 horizontal steps each 0.61m high and 1.22m long. The discharge was varied from 0.57 to 3.28 m^3/s. The data series obtained for model comparison include; velocity profiles, air concentration, and characteristics of flow. Both models can satisfactorily simulate the flow pattern and the recirculation regions. The velocity profiles are more accurately simulated using the VOF model. The MMF model gave satisfactory results for air concentration.

1 INTRODUCTION

In recent years, there has been an increase in the rate of surplus or flood waters which cause high flow into the reservoirs. Due to the increase of water flow, the storage capacity may be exceeded. The dam spillways must be designed to release surplus or flood water and to avoid exceeding reservoir capacity., Gonzalez and Chanson (2006) mentioned higher design flows that affect the insufficiency of the existing spillway capacity. A spillway is kind of hydraulic structure that is provided at storage and detention dams to release water that cannot be safely stored in the dam (Tabbara et al., 2005). To be safe, the spillway must be capable of passing high flow without jeopardizing the dam. A stepped spillway is an important kind of spillway having profile made up of steps. It dissipates much more energy than other types of spillways when water is flowing over the spillway profile. According to Chanson (1994), stepped spillways have been used for at least 1500 years. Historically, very active experimental research has been done on the air-water flow over stepped spillways, such as flow patterns, inception of air entrainment, air concentration, velocity field, pressure field and energy dissipation (Qian et al., 2009). The engineers have normally investigated the flow through laboratory experiments on scaled down models of spillways. The complexity of the flow structure which includes complicated boundary conditions, the curved free surface, and the unknown scale effects has caused uncertainties in transposing the experimental results to prototype scales. With the development of computational fluid dynamics (CFD) and high-performance computers, complex multiphase flows can be simulated numerically and with validation the results can be trusted to be reliable. Given reduced time demand and lower cost of the numerical method than physical experiments, simulation of the stepped spillway overflow has a significant advantage.

The two well established and widely used computational methods are the finite difference and finite element methods. Tabbara et al. (2005) used the finite element method to predict stepped flows at the small scale of experiments. In the upper part of the flume as well as in the bottom part steps were

introduced along the chute such that the envelope of their tips followed the smooth spillway chute profile. Although the results of this study are encouraging, physical or laboratory measurements are still crucial for providing reference data. Benmamar et al. (2003) developed a numerical model for two-dimensional boundary layer flow over a stepped channel with steep slope, which was based on the implicit finite difference scheme. The finite volume method, which has been extensively used to model a wide range of fluid-flow problems, was originally developed as a special finite difference formulation. Quian et al. (2009) used a MMF model to simulate flows over a stepped spillway. The turbulence models he investigated are realizable k-ε model, SST k-ω model, v^2-f model and LES model. There were 40 steps with the step height of 0.05 m. The study region comprised the 6^{th} to 12^{th} steps from the crest. The realizable k-ε model is the most efficient in simulating flow over stepped spillways. Dong (2006) studied numerical simulation of skimming flow over mild stepped channel. The channel he investigated consisted of 40 steps with $\theta = 10^o$ and 20^o. All air boundaries were defined as pressure boundaries with zero pressure specified. Smooth channel flow was also simulated to compare the hydraulic characteristics of the stepped channel flow with the smooth one. Chen (2002) used the k - ε turbulence model to simulate the complex turbulence overflow. Their first five steps were varied while the size of the rest were 0.06 m high and 0.045 m long. The study indicated that the turbulence numerical simulation is an efficient and useful method for the complex stepped spillway overflow.

All of the previous studies focused on the small scale stepped spillways and tested discharge. Tabbara et al. (2005) mentioned about the relationship and advantage of numerical model, there should be calibrating and verifying the numerical model with the large scale experiments. Therefore, large scale of stepped spillway is studied for both experiments and numerical model. Also due to less time demand and lower cost of the numerical method than that of experiments, this study will be emphasized on numerical model to attest that numerical model can be used compared with large scale experiments. The flow pattern and flow characteristics, flow profiles along the spillway, velocity profiles, and air concentration profiles, were collected from the experiments which consist of nappe flow and skimming flow. The VOF and MMF were used as a multiphase flow model to compare the better one using with large scale experiments.

2 NUMERICAL MODEL

FLUENT is used in this study for both solver and post-processing. It is a software tool for general purpose CFD. The stepped spillway was modeled as shown in Fig.1. For each case studied, there are 230,565 quadrilateral cells with 232,109 nodes created. Quadrilateral meshes with 0.1×0.1 m are used. The boundary conditions in this study are no-slip wall as a wall type, outlet as a pressure outlet type, free surface as a pressure inlet type, air inlet and water inlet as a velocity inlet type. The inlet water velocity is set as uniform at the inlet. Then water flows into the tank before approaching the spillway. The segregated solver was used because it is multiphase flow with 2 materials, water and air, each with different velocity. The VOF and/or MMF models were used to deal with the multiphase fluids..

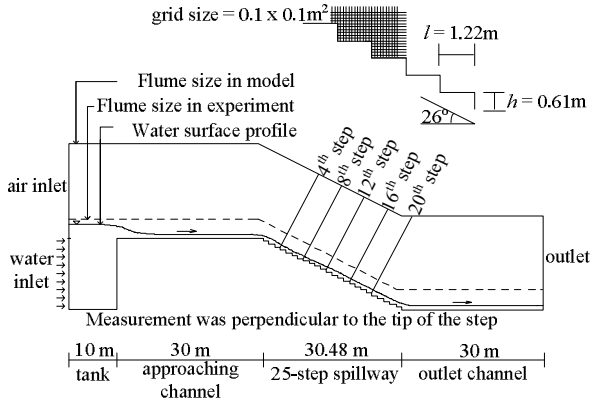

Figure 1. Schematic diagram of the stepped spillway

2.1 The volume of fluid model (VOF)

The VOF formulation relies on the fact that two or more phases are not interpenetrating. In each control volume, the volume fractions of all phases sum to unity. The fields for all variables and properties are shared by the phases and represent volume-averaged values, as long as the volume fraction of each of the phases is known at each location. Thus the variables and properties in any given cell are either purely representative of one of the phases, or representative of a mixture of the phases, depending upon the volume fraction values. In the geometric reconstruction approach, the standard interpolation schemes are used to obtain the face fluxes whenever a cell is completely filled with one phase or another. When the cell is near the interface between two phases, the geometric reconstruction scheme is used. It assumes that the interface between two fluids has a linear slope within each cell, and uses this linear shape for calculation of the advection of fluid through the cell faces. The first step in this

reconstruction scheme is calculating the position of the linear interface relative to the center of each partially-filled cell. The second step is calculating the advecting amount of fluid through each face using the computed linear interface representation and information about the normal and tangential velocity distribution on the face. The third step is calculating the volume fraction in each cell using the balance of fluxes calculated during the previous step.

A single momentum equation is solved throughout the domain, and the resulting velocity field is shared among the phases. The momentum equation, eq.(1), is dependent on the volume fractions of all phases through the properties ρ and μ.

$$\frac{\partial}{\partial t}(\rho\vec{v})+\nabla\cdot(\rho\vec{v}\vec{v}) = -\nabla p+\nabla\left[\mu\left(\nabla\vec{v}+\nabla\vec{v}^{T}\right)\right]+\rho\vec{g}+\vec{F} \quad (1)$$

The limitation of the shared-fields approximation is that in cases where large velocity differences exist between the phases, the accuracy of the velocities computed near the interface can be adversely affected. The energy equation, also shared among the phases, is

$$\frac{\partial}{\partial t}(\rho E)+\nabla\cdot\left(\vec{v}(\rho E+p)\right)=\nabla\cdot\left(k_{eff}\nabla T\right)+S_h \quad (2)$$

$$E=\frac{\sum_{q=1}^{n}\alpha_q\rho_q E_q}{\sum_{q=1}^{n}\alpha_q\rho_q} \quad (3)$$

2.2 The mixture multiphase flow model (MMF)

The MMF model is suggested to use for bubbly flows and pneumatic transport. It is a simplified multiphase model that can be used where the phases move at different velocities, but assume local equilibrium over short spatial length scales. The coupling between the phases should be strong. It can also be used to model homogeneous multiphase flows with very strong coupling and the phases moving at the same velocity. The mixture model can model *n* phases by the continuity equation for the mixture, the momentum equation for the mixture, the energy equation for the mixture, and the volume fraction equation for the secondary phases, as well as algebraic expressions for the relative velocities. The continuity equation for the mixture is

$$\frac{\partial}{\partial t}(\rho_m)+\nabla\cdot(\rho_m\vec{v}_m)=0 \quad (4)$$

$$\vec{v}_m=\frac{\sum_{k=1}^{n}\alpha_k\rho_k\vec{v}_k}{\rho_m} \quad (5)$$

$$\rho_m=\sum_{k=1}^{n}\alpha_k\rho_k \quad (6)$$

The momentum equation for the mixture can be obtained by summing the individual momentum equations for all phases.

$$\frac{\partial}{\partial t}(\rho_m\vec{v}_m)+\nabla\cdot(\rho_m\vec{v}_m\vec{v}_m) = -\nabla p+\nabla\cdot\left[\mu_m\left(\nabla\vec{v}_m+\nabla\vec{v}_m^{T}\right)\right]+\rho_m\vec{g} + \vec{F}+\nabla\cdot\left(\sum_{k=1}^{n}\alpha_k\rho_k\vec{v}_{dr,k}\vec{v}_{dr,k}\right) \quad (7)$$

$$\mu_m=\sum_{k=1}^{n}\alpha_k\mu_k \quad (8)$$

$$\vec{v}_{dr,k}=\vec{v}_k-\vec{v}_m \quad (9)$$

The energy equation for the mixture takes the following form

$$\frac{\partial}{\partial t}\sum_{k=1}^{n}(\alpha_k\rho_k E_k)+\nabla\cdot\sum_{k=1}^{n}\left(\alpha_k\vec{v}_k(\rho_k E_k+p)\right) = \nabla\cdot\left(k_{eff}\nabla T\right)+S_E \quad (10)$$

where k_{eff} is $\sum\alpha_k(k_k+k_t)$ defined according to the turbulence model being used.

$$E_k=h_k-\frac{p}{\rho_k}+\frac{v_k^2}{2} \quad (11)$$

The differences between the models are the manner in which they handle phase interpenetration and the phase velocities. With these two differences, the initial boundary condition must be different. The air velocity in mixture model should be set at zero and then reduced to homogeneous multiphase model while the air velocity in VOF model should be the same as water velocity. Flow over different kinds of spillways produce different patterns and have different effects.

For operating conditions, the specified operating density, 1.225 kg/m^3, was used with gravitational acceleration, -9.81 m/s^2, and operating pressure 101,325 Pa. The boundary conditions were set by using water velocity at water inlet. The Realizable *k*-ε model, with non-equilibrium wall functions, was used to simulate turbulence. The default values of model constants were used. It is a relatively recent development from the standard *k*-ε model. A new transport equation for the dissipation rate, ε, has been derived from an exact equation for the transport of the mean-square vorticity fluctuation. An immediate benefit of the realizable *k*-ε model is that it more accurately predicts the spreading rate of both

planar and round jets. The modeled transport equations for k and ε in the realizable k-ε model are

$$\frac{\partial}{\partial t}(\rho k)+\frac{\partial}{\partial x_j}(\rho k u_j) = \frac{\partial}{\partial x_j}\left[\left(\mu+\frac{\mu_t}{\sigma_k}\right)\frac{\partial k}{\partial x_j}\right]+G_k+G_b-\rho\varepsilon-Y_M+S_k \quad (12)$$

$$\frac{\partial}{\partial t}(\rho\varepsilon)+\frac{\partial}{\partial x_j}(\rho\varepsilon u_j)=\frac{\partial}{\partial x_j}\left[\left(\mu+\frac{\mu_t}{\sigma_\varepsilon}\right)\frac{\partial\varepsilon}{\partial x_j}\right] + \rho C_1 S_\varepsilon-\rho C_2\frac{\varepsilon^2}{k+\sqrt{\upsilon\varepsilon}}+C_{1\varepsilon}\frac{\varepsilon}{k}C_{3\varepsilon}G_b+S_\varepsilon \quad (13)$$

where $C_1=\max\left[0.43,\frac{\eta}{\eta+5}\right], \eta=S\frac{k}{\varepsilon}, S=\sqrt{2S_{ij}S_{ij}}$

The under-relaxation factors are used in the pressure-based solver to stabilize the convergence behavior of the outer nonlinear iterations by introducing selective amounts of ϕ in the system of discretized equations. Four under-relaxation factors, i.e. pressure coefficient, momentum coefficient, k, and ε, are set to default values, 0.3, 0.7 0.7, and 0.8, respectively. The default values are near optimal for the largest possible number of cases. For the time step size, 0.5s was used for every case. The implicit equation can be solved iteratively at each time level before moving to the next time step. The advantage of the fully implicit scheme is that it is unconditionally stable with respect to time step size. However, the Courant number that is used for stability checking is set at 0.25 which is less than 1.0 and stable.

3 EXPERIMENTS

The experiments were obtained using an outdoor testing facility located at Colorado State University Engineering Research Center. The facility permits large scale experiments so the water was supplied from nearby Horsetooth Reservoir. The test facility includes a water supply pipeline, baffled head box, entrance, concrete chute, stilling basin, and outlet works. The concrete chute is approximately 34.14 m long, 1.22 m wide, and 1.52 m deep on a 2:1 (horizontal: vertical) slope and has a total height of 15.24 m. Plexiglas windows with the size of 1.22 m by 1.22 m were installed at five locations in the dividing wall to provide observation of flow in the chute. Water was supplied through a 0.91 m diameter pipeline approximately 0.8 m long. At the maximum reservoir elevation, the facility is capable of direct discharge up to 3.4 m^3/s. A sonic flow meter in the supply pipeline to the facility head box was used to monitor flow in the system.

The spillways consisted of twenty-five horizontal steps with height, h = 0.61 m and length, l = 1.22 m. Flow discharges of 0.57, 1.13, 2.83, and 3.28 m^3/s were used. Data collected, included: flow rate, overtopping head, air concentration profiles, and velocity profiles, which were measured at five locations along the spillway. The data on the 4th, 8th, 12th, 16th, and 20th steps were measured, perpendicular to the spillway floor as shown in Fig.1, from a designated reference datum to the point of data collection. The reference datum is located at the first step, perpendicular to the spillway floor.

Air concentration and velocity instrumentation were mounted on a point gage and carriage system. The manually operated carriage system allowed for two degrees of freedom with movement along the length of spillway parallel to the floor, and lateral movement within the width of the spillway. The remote operated, motorized point gage allowed for vertical movement of the instrumentation perpendicular to the floor of the spillway to obtain data profiles within the flow. All profiles were taken along the centerline of the flume (0.61 m lateral distance from the wall) normal to the spillway floor. Each profile consisted of anywhere from 3 to 30 data points depending upon the depth of flow and reading interval chosen. The lowest points were taken at approximately 0.015 m from the tip of the step. The highest points were taken where both instruments measured data that was near the dry-air readings and visually appeared almost out of the flow.

3.1 Velocity measurement

Videotape recording and photographs were used to collect the flow pattern at the overtopping crest and along the spillway. Flow condition in this study may be described as high-velocity, turbulent, two-phase flow. Therefore, a probe to measure velocity was required that would withstand high impact forces and be able to accommodate a nonhomogeneous fluid of varying density. The probe is sturdy and provides a means of continuous back flushing to ensure a single density fluid within the Pitot tube. Velocity from the back-flushing Pitot tube is determined by the difference in pressures at the kinetic and static ports while continuously back flushing to prevent air bubbles from entering the instrument. Therefore, a balance between ensuring that air does not enter the Pitot tube and the sensitivity of the pressure difference must be found.

3.2 Air concentration

For the term “air concentration”, many theories of self-aerated flow suggest the flow depth is divided

into at least two regions. The lower region consists of water containing individual air bubbles distributed throughout the flow and exchanged with the upper region. The upper region contains a wavy water surface in which air is trapped or sounded by waves and other breaks in the surface. Based on this theory, there is the distinction between entrained air and entrapped air. Entrapped air in the upper region is transported in the trapped region of the irregular, wavy surface. Entrained and entrapped air together make up the total air transported with the flow.

The air concentration probe was used to determine the percentage of air contained in flow. The principle for air concentration measuring is based on the difference in electrical resistivity between air and water. The probe act as a bubble detector by passing a current through two conductors spaced a small distance apart and measuring the change in conductivity that occurs when a bubble impinges on the probe tip. The interruption of the current when a bubble passes is a step change from a relatively high conductivity with the probe in water, to nearly zero conductivity when a bubble breaks the conducting path. Integrating this signal over time gives the probability of encountering air. The air probe consists of two platinum wires as conductors, separated by approximately 2.0 mm. The wires are encased in a non-conducting acrylic tip and fit into a 6.35mm stainless steel supporting tube.

4 RESULTS AND DISCUSSION

4.1 Flow characteristics on step

For the flow regime, Chinnarasri and Wongwises (2004) proposed the minimum critical flow depth required for the onset of skimming flow on horizontal and inclined steps for $0.10 \le \frac{h}{l} \le 1.73$ is

$$\frac{y_c}{h} = (0.844 + 0.003\theta)\left(\frac{h}{l}\right)^{-0.153+0.004\theta} \quad (13)$$

The maximum critical flow depth for the nappe flow regime is

$$\frac{y_c}{h} = 0.927 - 0.005\theta - 0.388\left(\frac{h}{l}\right) \quad (14)$$

For the present study, at 0.57 m^3/s and $\frac{y_c}{h} = 0.46$, nappe flow existed with ponded water in the interior of the step beneath a cascading free jet. At 1.13 m^3/s, with $\frac{y_c}{h} = 0.73$, partial impact of the flow near the end of step and incomplete filling of the step cavity suggest a partial nappe flow regime. The condition of skimming flow was first observed at 0.37 m^3/s or greater. Therefore, the flow regime at discharges of 2.83 and 3.28 m^3/s, which $\frac{y_c}{h} = 1.34$ and 1.48, respectively, were skimming flow. The complete submergence of the steps with water flowing down the slope as a coherent stream cushioned by recirculating vortices in the interior of the step was found. However, the general flow conditions were extremely turbulent along the entire spillway with erratic flow patterns and significant splash occurring at all flow rates. The details of each case are summarized in the Table 1.

Total discharge (m^3/s)	Critical depth (m)	$\frac{y_c}{h}$	Flow regime
0.57	0.28	0.46	Nappe
1.13	0.45	0.73	Nappe
2.83	0.82	1.34	Skimming
3.28	0.91	1.48	Skimming

Table 1. Details of the tests

Non-aerated flow existed prior to the crest of the first step with surface aeration initiating immediately thereafter. For large flows, aeration was observed to continue immediately after the first step, however, a fully aerated flow profile was not observed until between the 2nd and 3rd step downstream from the entrance of the spillway. The flow on the 16th step is used to show the observation because it is located in the middle zone of spillway, which is assured that flow in that zone is uniform flow. The nappe flow and skimming flow on the 16th step from the MMF model are shown in the Fig.2A and B, respectively.

The flow direction, and location of the recirculating vortices on the step from the simulation both from VOF and MMF models are similar. There are two zones; lower and upper zones, along the spillway. Closing to the step is lower zone with the recirculating vortices rotates clockwise and is located in the triangular zone of the step corner. The upper zone is far from the step and drops of water flow through the air. The results for the MMF model calculations can separate the air from the water flow so the connected surface between air and water can be seen clearly and the flow direction of water flow can be shown. The connected surface from the VOF model cannot be seen clearly because of the processes inherent solutions derived solved during the volume fraction method. The flow direction of mixture is shown instead of a separation between air and water.

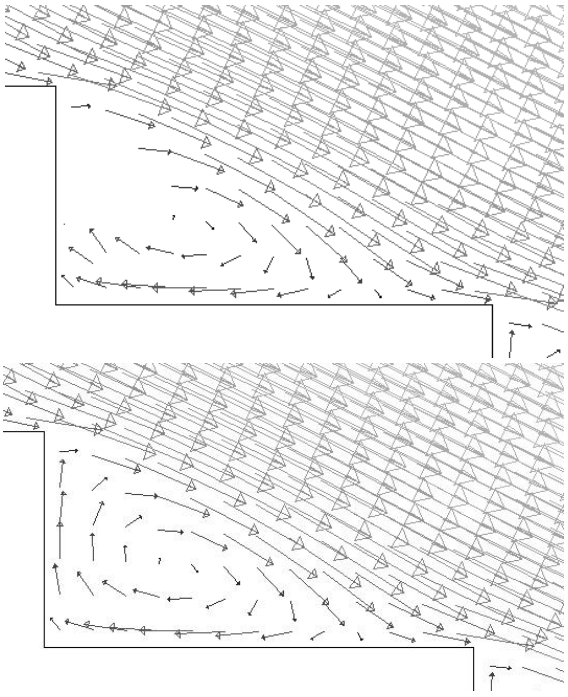

Figure 2. Flow characteristics on the 16th step from MMF

4.2 Flow pattern

Flow down along the stepped spillway involves highly turbulent self-aerated flows. An important flow characteristic was observed in the transverse cross sectional surface flow pattern viewed from above. A distinct "U" shape of surface aeration was often noted near the crest and along the entire length of the spillway indicating resistance along the walls and a uniform velocity distribution across the flume. For the skimming flow regime, waves formed along the sidewalls that appeared to slightly super elevate the water surface from which the waves would collapse or roll into the main flow. The highest velocity region was observed to be located in the center of the cross section.

The flow profiles of skimming flow from both VOF and MMF models are similar. The flow profiles along the stepped spillway from VOF model is shown in the Figure3.

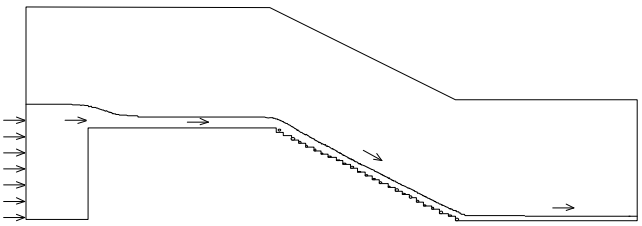

Figure 3. Flow profiles of skimming flow from VOF model

Similarly to the flow profiles from the experiments, the water depth from the model slightly decreases with distance, reflecting the profiles of velocity, especially for higher flow rates. From the experiments, the point of interception, which is the point of separation between non-aerated flow, flow without air, and self-aerated flow, flow with air bubbles inside are shown and clearly seen. It cannot be seen from the VOF model results. Even though there is the volume fraction calculation in MMF model, this point still cannot be seen clearly, since there is only percentage of air concentration provided by the results. The point of interception can be predicted by MMF model but it is still not the accurate point. On the other hand, the VOF displays the recirculation vortices on the step while it cannot be seen for the MMF model results.

4.3 Velocity profiles

For the velocity profiles tend to have the same shape beginning with velocity gradually increasing from the bed until a maximum velocity gradient is reached. At some point in the upper region of the depth, an immediate change is observed where the velocity abruptly increases or decreases. Velocity profiles similar to this shape have been observed in several studies of stepped spillway flow (Chamani and Rajaratnam, 1999). Straub and Lamb (1956) first mentioned and noticed the phenomenon in velocity measurements in the upper region. Flow conditions in the upper region consisted of a highly irregular, wavy surface above which large particles of water ejected from the main flow. It was hypothesized that shear stress develops from increased resistance on these particles due to atmospheric drag and the change in momentum and the return of particles back to the main flow results in a loss of velocity.

For both nappe flow and skimming flow, the VOF model shows better agreement with measurements compared to the MMF model. The velocity profiles for the discharges of 0.57 m^3/s, nappe flow, and 3.28 m^3/s, and skimming flow on the 16th step are shown in the Figure 4.

A comparison of the velocity results from the numerical model and experiments shows that with a nappe flow regime, the maximum error in their values mainly amount to 30% in the zone upper when 0.10 m from the floor bed of the spillway. For a skimming flow regime lower than 0.20m, the error is quite high as well as the one from nappe flow while the maximum error is not more than 27% in the upper zone. Given the grid size of 0.1×0.1 m^2 for the numerical model with the finite volume method, the maximum error is from the point that is located on the center of the cell, at 0.05 m. The results of the

lower zone, therefore, are interpolated from the boundary of the cell. With this reason, the error from the floor to the depth 0.20 m is quite high.

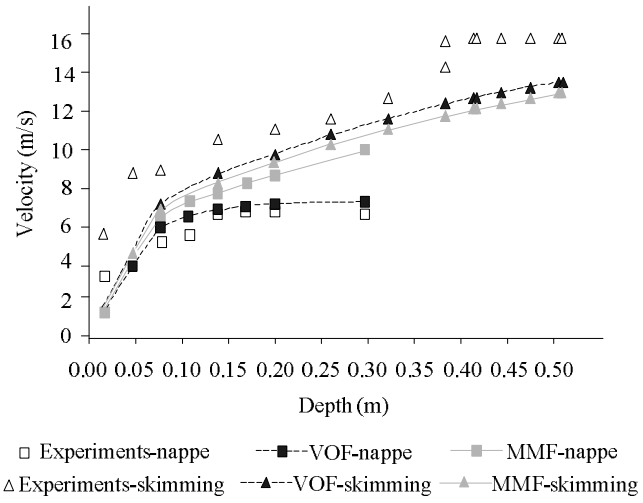

Figure 4. Velocity profiles on the 16th step

4.4 Air concentration

On the flows down stepped spillway, Ruff and Frizell (1994) defined the characteristic depth as the perpendicular distance from the pseudo-bottom, $y_{0.9}$, formed by the step edges where the air concentration is 90%, It was found to underestimate considerably the maximum height of large air-water mass projections. The Air concentration profiles consisted of local air concentration values obtained along the characteristic depth. Trends exhibited in the air concentration profile curves from this study are typical of those found on stepped spillway models using similar instrumentation (Boes and Hager, 1998). For this study, flow conditions in the nappe flow regime exhibit a less defined lower and middle region. As a discharge increases, apparent depth increases with the shape of the curve remaining fairly constant. Flow conditions in the skimming flow regime showed air concentration increasing gradually from the bed and more rapidly in the middle region of the profile. Near the surface, the change in air concentration with depth begins to decrease prior to reaching the surface. This is a distinct difference that can be noted in the shape and slope of the curves at 0.57 and 1.13 m^3/s compared to 2.83 and 3.28 m^3/s.

As noted above, the important point of interest that is always used in design of stepped spillways is $y_{0.9}$. At the point $y_{0.9}$, the air concentration for nappe flow from the MMF model agrees better with the results from experiments while for the skimming flow the agreement is not as satisfactory.

The air concentration profiles for the nappe flow and skimming flow on the 16th step are shown in the Figure 5. For the numerical model, there is an interaction of the inter-phase mass, momentum and energy transfer in the MMF model while the VOF method does not compute the dynamics in the void or air regions. The trends of results using VOF look good from the starting point because the values of air concentration are very low. After that, the MMF model results are better. The best point of simulation is at $\frac{y}{y_{0.9}} \approx 0.66$ for both nappe flow and skimming flow.

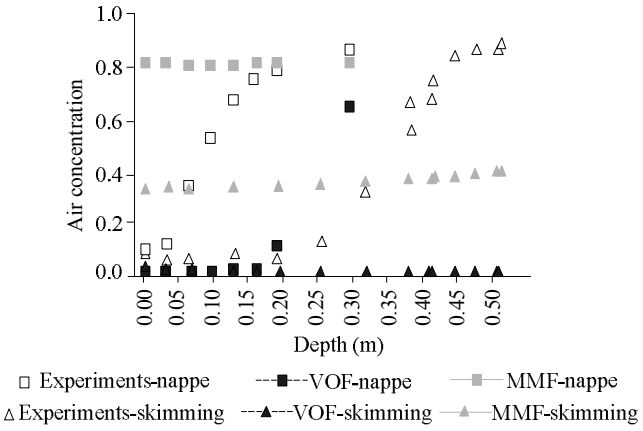

Figure 5. Air concentration on the 16th step.

5 CONCLUSIONS

A numerical model using different multiphase flow models, VOF and MMF model, is used to study and compare the flow over a stepped spillway. The data from large-scale experiments are used to calibrate and verify the model. The 25 step spillway with the step size of 0.61 m high and 1.22 m long is used. The discharges of 0.57, 1.13, 2.83, and 3.28 m^3/s were used. For the first two discharges, the nappe flow regime is found while the skimming flow regime is found for the rests. The commercial software FLUENT is used as a computational fluid dynamics method. The grid size used quadrilateral meshes of 0.1×0.1 m^2. For nappe flow, there is no recirculating vortex on the step. There is only an air pocket which is not clearly seen from the model. According to the simulation results for skimming flow, it is obvious that there is a recirculating vortex in the corner of the step, which is called lower zone, verified by the measurements. The upper zone is a wavy water surface in which air is trapped in the surface. To simulate the flow characteristics on the step, MMF model is better used. MMF is also preferred to simulate the flow pattern along the spillways. The point of interception can be found in

MMF model but without recirculating vortices shown on the step.

For the velocity profiles, they tend to have the same shape beginning with velocity gradually increasing from the bed until a maximum velocity gradient is reached. For both nappe flow and skimming flow, the VOF model shows better agreement compared to the MMF model. The maximum error in their values was 30% in the zone greater than 0.10 m from the floor bed of the spillway. For a skimming flow regime, the maximum error is not more than 27% in the upper zone.

The air concentration is not well simulated in this study. There is high error for both VOF and MMF models. However, the VOF model always underestimated the value of air concentration while the MMF model is better simulating the flow. There is an interaction of the inter-phase mass, momentum and energy transfer in the MMF model while the VOF method does not compute the dynamics in the void or air regions. The best point of simulation by MMF model is at $\frac{y}{y_{0.9}} \approx 0.66$ for both nappe flow and skimming flow.

6 ACKNOWLEDGEMENT

The authors would like to thank the Thailand Research Fund/Royal Golden Jubilee PhD Grant (TRF/RGJ) for providing financial support under grant number (Grant no. PHD/0225/2548) for this study.

7 NOTATION

The following symbols are used in this paper:

C = constant
E = energy
E_q = energy based on the specific heat
F = body force
g = gravitational acceleration
G = generation of turbulent kinetic energy
h = step height
h_k = sensible enthalpy for phase k
k = turbulent kinetic energy
k_{eff} = effective thermal conductivity
k_t = turbulent thermal conductivity
l = step length
p = pressure
S_E = volumetric heat sources
S_h = source term
t = time
T = temperature
u_j = velocity component
v = velocity
$\vec{v}_{dr,k}$ = drift velocity for secondary phase k
$\vec{v}_k$ = velocity for phase k
$\vec{v}_m$ = mass-averaged velocity
x_j = coordinate component
y_c = critical depth
α_k = volume fraction of phase k
α_q = volume fraction based on the specific heat
ε = turbulent dissipation rate
μ = molecular viscosity
μ_m = viscosity of the mixture
μ_t = turbulence viscosity
ρ = mass density of fluid
ρ_k = mixture density
ρ_m = mixture density
ρ_q = mass density of fluid based on the specific heat
σ_ε = turbulence Prandtl number for ε
σ_k = turbulence Prandtl number for k
θ = angle of the upward inclined step in degrees

8 REFERENCES

Benmamar, S., Kettab, A. and Thirriot, C. 2003. Numerical simulation of turbulent flow upstream of the inception point in a stepped channel. *Proceedings, 30th IAHR Congress.* Auth, Thessaloniki, Greece: 679-686

Boes, R.M.& Hager, W.H. 1998. Fiber-optical experimentation in two-phase cascade flow. *Proceedings of the International RCC Dams Seminar*, K.Hansen (ed), Denver

Chamani, M.R.& Rajaratnam, N. 1999. Characteristics of skimming flow over stepped spillways. *Journal of Hydraulic Engineering* 125(4)

Chanson, H. 1994. Hydraulics of skimming flows over stepped channels and spillways. *Journal of Hydraulic Research* 32(3)

Chen, Q., Dai, G. & Liu, H. 2002. Volume of fluid model for turbulence numerical simulation of stepped spillway overflow. *Journal of Hydraulic Engineering* 128(7): 683-688

Chinnarasri, C. & Wongwises, S. 2004. Flow regimes and energy loss on chutes with upward inclined steps. *Canadian Journal of Civil Engineering* 31(5): 870–879

Dong, Z.Y. & Lee, J.H. 2006. Numerical simulation of skimming flow over mild stepped channel. *Journal of Hydrodynamics Series B* 18(3): 367-371

Gonzalez, A.C. & Chanson, H. 2006. Air entrainment and energy dissipation on embankment spillways. *Proceedings of the International Symposium on Hydraulic Structures, IAHR Symposium,* 12-13 October 2006, Ciudad Guayana, Venezuela.

Qian Z.D., Hu, X.Q., Huai, W.X. & Amador, A. 2009. Numerical simulation and analysis of water flow over stepped spillways. *Science in China Series E:Technological Sciences* 52(7): 1958-1965

Ruff, J.F. and Frizell, K.H. 1994. Air concentration measurements in highly-turbulent flow on a steeply-Sloping Chute"; *Proceedings of hydraulics engineering conference*, ASCE, Buffalo, N.Y., 999-1003

Straub, L.G. & Lamb, O.P. 1956. Experimental studies of air entrainment in open channel flow. *Proceedings, Minnesota International Convention,* Minneapolis, Minnesota, September.

Tabbara, M., Chatila, J. & Awwad, R. 2005. Computational simulation of flow over stepped spillways. *Computers and Structures* 83:2215–2224